Seismic Anisotropy in the Crust in Lateral Collision Zone of Southeast Margin of Tibetan Plateau by the Temporary SL-Array

Yuan Gao[1*], Anguo Chen[1], Tielong Guo[1], Yutao Shi[1], Ziqi Zhang[1] and Lanbo Liu[2]

[1] Institute of Earthquake Forecasting, China Earthquake Administration, Beijing 100036, China
[2] Department of Geosciences, University of Connecticut, Storrs, CT 06269, USA
[*] Correspondence to: Yuan Gao, qzgyseis@163.com; gaoyuan@cea-ies.ac.cn

JULY 8-18 JUILLET 2019 | MONTREAL, CANADA
27th IUGG General Assembly
Assemblée Générale de l'UGGI
IUGG Centennial | 1919-2019 | Centenaire de l'UGGI

Abstract Ref. No. IUGG19-1826
Presentation No. S10p-394

Abstract

With seismic data from a temporary Seismic Linear Array (the SL-Array), as well as permanent seismic stations, we obtained SWS parameters from local earthquakes and effective data derived from identification on microseismic events (IMSE) in the lateral collision zone in the southeast margin of the Tibetan Plateau. From west to east, the study area can be divided into three subzones. The fast polarization (i.e. polarization of fast shear-wave) varies gradually from NNW, NS to NNE in these three subzones. The time delay of the slow shear-wave (i.e. time difference between two split shear-waves) also increases clearly in the same direction order, indicating seismic anisotropy above 25 km depth in the crust. Both SWS parameters are closely related to stress, faults and tectonics. The scatter and the dual dominant orientations of the fast polarizations at some stations indicate strong disturbance from faults nearby or from deep tectonics. Anisotropic parameters are found to be related to the metallogenic belt to some degree. It is worth for further analyzing the link between them, suggesting that SWS could be applied to study metallogeny.

Station Distribution

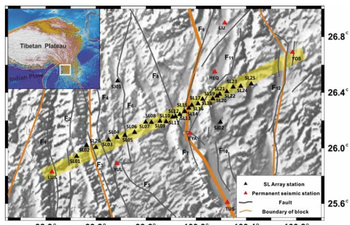

Fig 1. Seismic station distribution in the Sanjiang area. The black and red triangles indicate the temporary and permanent seismic stations, respectively. The linear profile within the yellow-color highlighted area is the temporary seismic array (the SL-Array), plus two permanent stations. The SJ01 and SJ02 are also temporary seismic stations of the SL-Array. The thick and thin brown lines indicate the 1st- and 2nd-order boundary of tectonic blocks, respectively. Faults: F1, west Nujiang Fault; F2, Nujiang Fault; F3, Caojian Fault; F4, Lancang River Fault; F5, Yongping Fault; F6, Lanping-Yunlong Fault; F7, Nanjian-Weishan Fault; F8, Weixi-Qiaohou Fault; F9, Zhongdian-Longpan-Qiaohou Fault; F10, Red River Fault; F11, Xiaojinhe-Lijiang Fault; F12-Chenghai Fault.

IMSE (Identification on microseismic events)

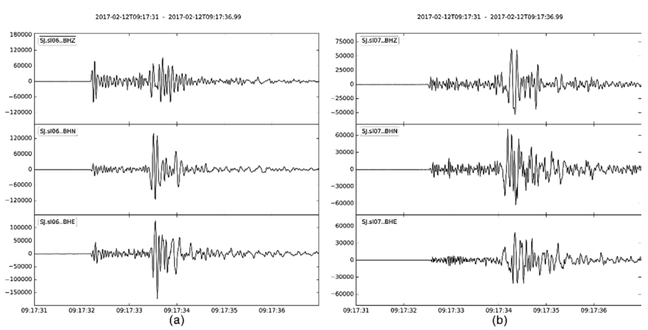

Figure 2. Seismic waveforms of a template event. The three-component seismic waveforms of the template event at station SL06 (a) and Station SL07 (b). The template event occurred on Feb. 12, 2017 with a local magnitude M_L1.7 and a focal depth of 9.0 km. The epicentral distances of SL06 and SL07 are 6.95 km and 10.70 km, respectively. Waveforms from the top to the bottom are vertical, NS and EW component, respectively. The abscissa (X axis) is time, and the ordinate (Y axis) is amplitude in counts.

Identification Results

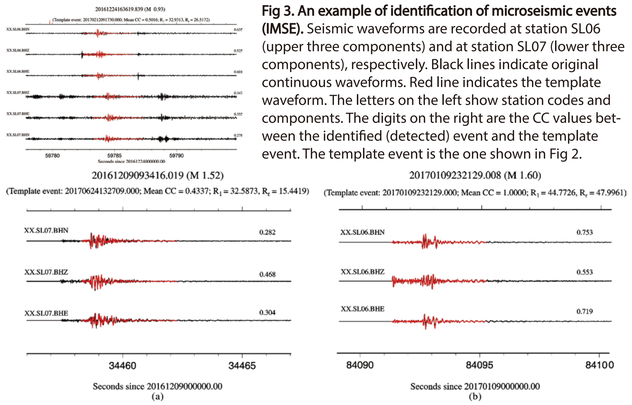

Fig 3. An example of identification of microseismic events (IMSE). Seismic waveforms are recorded at station SL06 (upper three components) and at station SL07 (lower three components), respectively. Black lines indicate original continuous waveforms. Red line indicates the template waveform. The letters on the left show station codes and components. The digits on the right are the CC values between the identified (detected) event and the template event. The template event is the one shown in Fig 2.

Fig 4. The IMSE test of two different template events. IMSE test results using two known earthquakes. The original continuous seismic waveforms and identified earthquake events are shown on the left at (a) station SL07 and on the right at (b) station SL06. Others are the same as in Fig 3.

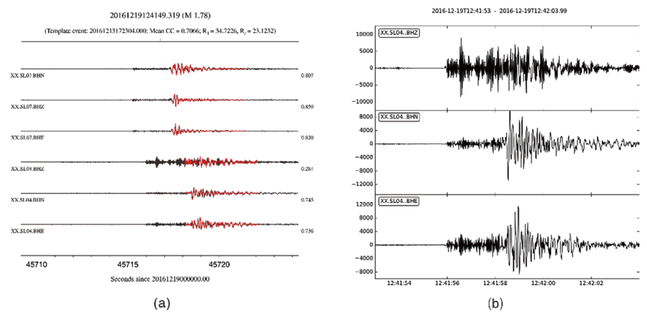

Fig 5. Template events and identified earthquake events. (a) Same earthquake event recorded at stations SL07 and SL04. Seismic waveforms are recorded at station SL07 (upper three components) and at station SL04 (lower three components), respectively. (b) The waveform of the identified earthquake event in three components at station SL04. The template event occurred at 17:23:04 on Dec. 13, 2016, location at 26.04°N, 99.56°E, magnitude M_L1.8, focal depth 14 km. The identified event occurred at 12:41:49 on Dec. 19, 2016, location at 26.00°N, 99.60°E, magnitude M_L1.78, focal depth 22 km. Others are the same as in Fig 3.

SWS Analysis Method

We employed the Systematic Analysis Method (SAM) (Gao et al., 1998, 2008). By the SAM analysis, the grid search technique is used to perform correlation calculation and polarization analysis. After the time-delay is subtracted, the polarization pattern is compared to the one without subtracting (or eliminating). Then the SWS parameters (fast polarization and time-delay) are finally obtained. Due to the total internal reflection of the shear-wave incident on the surface, the data used for SWS analysis need to meet the limitation of the shear-wave window. The shear-wave window in this study is 50° incident angle (Crampin and Peacock, 2005).

References and Acknowledgments

Gao, Y., Chen, A. G., Shi, Y. T., Zhang, Z. Q., and Liu, L. B. (2019). Crustal shear-wave splitting in Sanjiang lateral collision zone of the SE margin of Tibetan Plateau and its tectonic implications: preliminary results by the temporary seismic linear array. [submitted to] *Geophysical Prospecting*.

Supported by the National Key R&D Project of China (2016YFC0600302) and the National Natural Science Foundation of China (Project 41730212).

SWS Results and Analysis

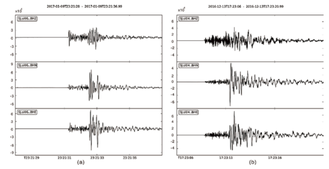

Fig 6. Seismic waveforms at two seismic stations. (a) Seismic waveforms of a small earthquake at station SL06. This earthquake occurred on Jan. 9, 2017, magnitude M$_L$1.6, focal depth 8.0 km, epicenter distance 7.13 km. (b) Seismic waveforms of a small earthquake at station SL04. This earthquake occurred on Dec. 13, 2016, magnitude M$_L$2.5, focal depth 18.0 km, epicenter distance 20.14 km. Others are the same as in Fig 2.

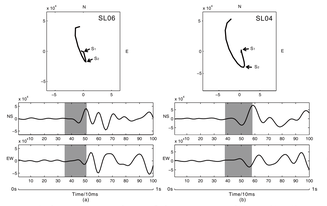

Fig 7. Polarization analysis of shear-wave splitting (SWS). (a) Records at station SL06. Lower is shear-waves of the two horizontal components. Abscissa (X axis) is number of sampling points. The sampling rate is 100 SPS (sampling points per second). Ordinate (Y axis) is amplitude in counts. Upper is polarization diagrams of shear-waves, where the plotted data correspond to the data of the shaded zone. S1 and S2 arrows points to the arrivals of the fast shear-wave and the slow shear-wave, respectively. (b) Records at station SL04. Others are the same as (a). Seismic records are the same as in Fig 6.

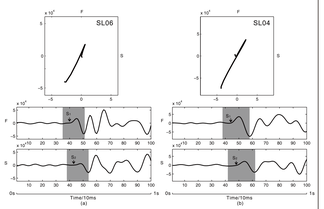

Fig 8. Polarization analysis of fast and slow shear-waves after eliminating time delay. All are the same as in Fig 7, after removing the time difference between the fast shear-wave and the slow one (i.e. time delay). (a) Station SL06, time delay is 0.03 s. (b) Station SL04, time delay is 0.04 s.

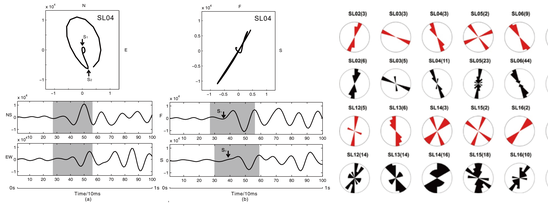

Fig 9. Example of SWS Analysis on identified microseismic events. The shear-wave records at station SL04 are same as in Fig 5. (a) polarization analysis of shear-wave splitting, similar to Fig 7. (b) polarization analysis of shear-wave splitting, similar to Fig 8. The fast polarization direction and the time delay are 152° and 0.03 s, respectively.

Fig 10. Fast polarizations of IMSE data in the SL Array. The upper rose diagrams (red) present fast polarizations of IMSE data. The lower rose diagrams (black) are those of all SWS data (ECR data plus IMSE data).

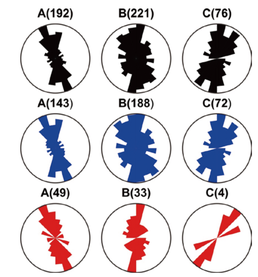

Fig 11. Rose diagrams of fast polarization directions in the three subzones. The letters above each equal-area project rose diagram are the subzone codes A, B and C (see Fig 12). The digitals in the brackets are numbers of effective SWS data in that subzone. The bottom (red) is fast polarizations of IMSE data. The middle (blue) is those of ECR data. The upper is those of IMSE data plus ECR data.

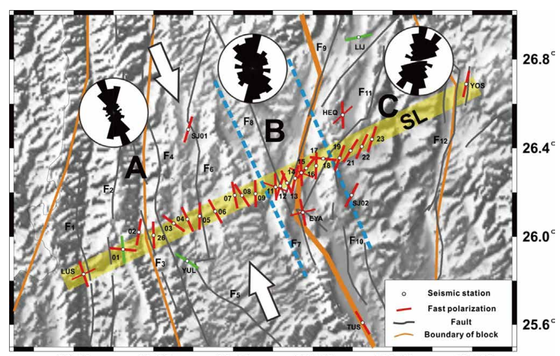

Fig 12. Spatial pattern of average fast polarization diretions in stations and dominant polarization diretions in the three subzones. The short line segments (red and green) are the average fast polarization direcitons at individual stations. The red color means that the number of SWS data are more than 2. The green color means that the number of SWS data is 2 or scatter of fast polarizations. The thick broken light-blue lines are the boundaries between the subzones. The pair of large arrows represent the regional maximum principal compressive stress direction (Cheng et al., 2003). The three rose diagrams show the fast polarizations in these three subzones, the same as those in the top line in Fig 11. Others are the same as in Fig 1.

Conclusions

Table. SWS parameters in three subzones in Sanjiang zone.

Subzone	No. of Effective Records	Fast polarizations ± errors /(°)	Normalized time delays ±errors /(ms·km^{-1})
A	192	160±27	1.0±0.8
B	221	179±42	1.6±1.7
C	76	30±36	1.9±2.0

▲ Dominant orientations of fast polarization directions are parallel to the direction of the regional principal compressive stress. Mean polarization direction changes from NNW, NS to NNE from the west to the east. In the study area, the scatter and the dual dominant orientations of fast polarization directions indicate strong disturbance of anisotropy from faults or deep tectonics. The results show that the dominant orientations of fast polarizations are consistent with the principal compressive strain, too.

▲ Time delays are different in the three subzones. Time delay is the smallest in subzone A in the west and the largest is in subzone C in the east. It indicates that the spatial anisotropic distribution is varying from west to east. SWS parameters in this paper show seismic anisotropy in the depth range above 25 km.